Supplementary Materials

Figure S 1

A

B   UPN#14

C

UPN#14

UPN#15
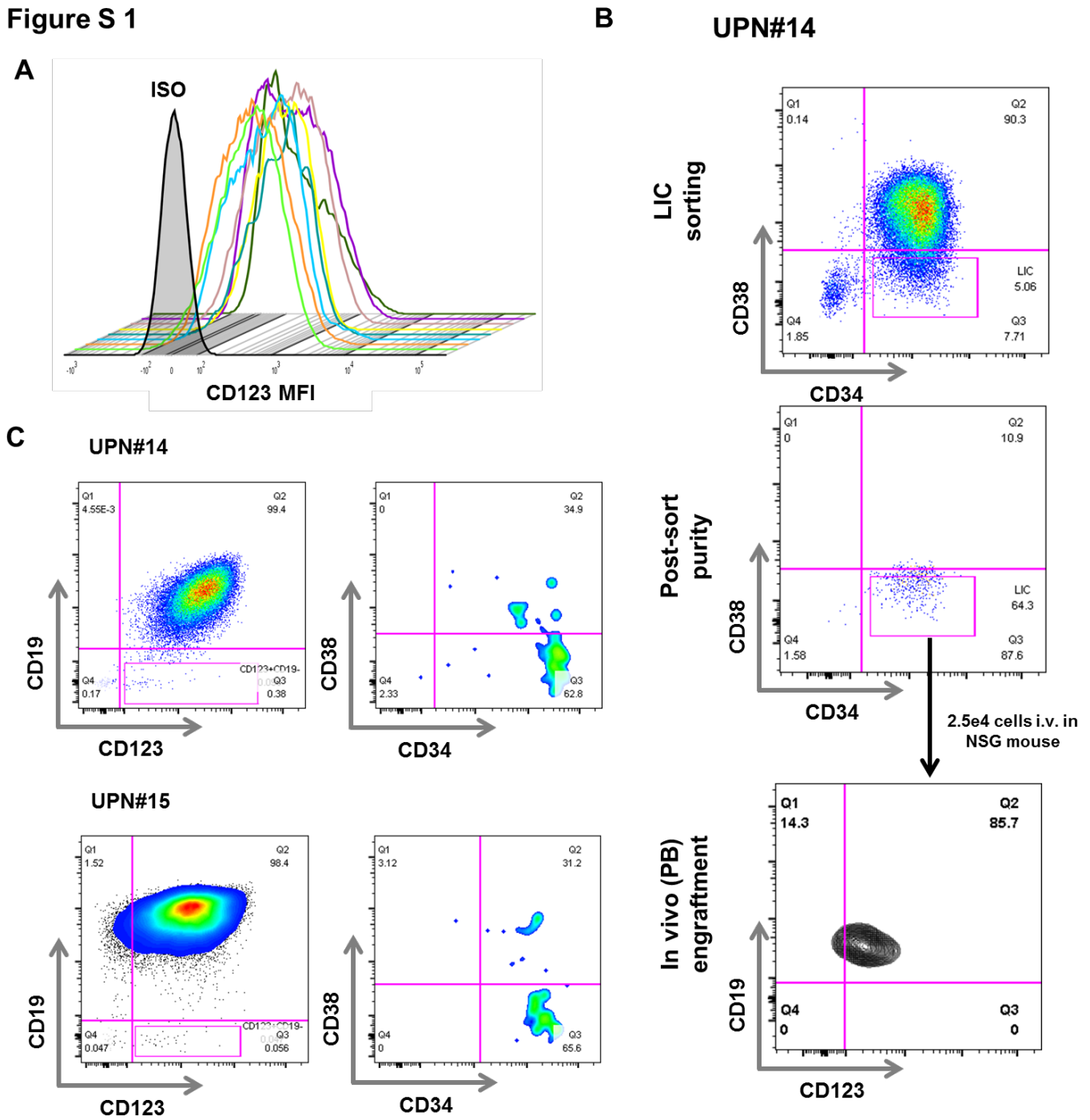
Figure S1. CD123 in acute lymphoblastic leukemia and leukemia-initiating cells. A. CD123 (histograms) is highly and homogenously expressed in B-ALL blasts (as defined by live, single, CD45dim cells) (8 representative cases shown). **B.** In order to confirm their LIC properties, CD34+CD38- leukemic blasts were sorted and injected in NSG mice. Peripheral blood analysis at day 37 revealed engraftment of CD45dim, CD19+, CD123+ human leukemic blasts. **C.** Leukemic blasts were analyzed by flow cytometry; the minor CD123+CD19- sub-populations demonstrated a LIC-like phenotype (CD34+CD38-). Each figure representative of at least two independent experiments.
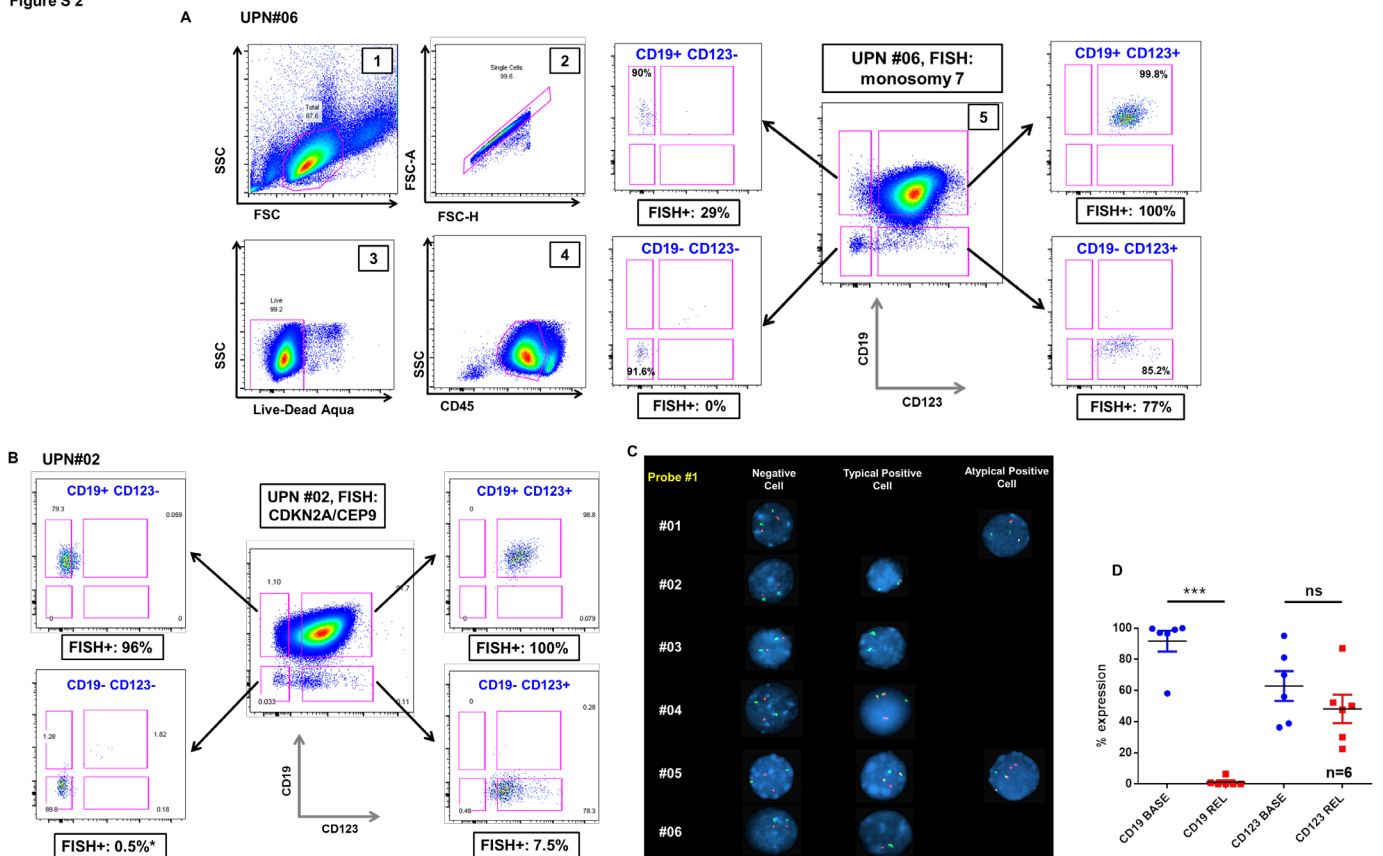
Figure S2. Expression of CD123 in the leukemia-initiating cell (LIC) and in CD19-negative relapses. A. The gating strategy and the sorting purity for patient shown in Fig. 1 D (UPN#06); leukemic blasts were defined as live, single, CD45dim, SSC low cells and four subpopulations, were sorted based on CD19 and CD123 expression. **B.** Another representative ALL sample (UPN#02) that was sorted and analyzed by FISH is shown here (same gating strategy as panel A). **C.** A FISH-positive and a -negative representative cells are shown for each ALL patient analyzed. Patient UPN#03 and #05 showed also atypically positive cells. *=considered negative **D.** CD123 expression is maintained in 6 B-cell acute lymphoblastic leukemia patients relapsing with CD19-negative disease after CLT019 (CART19) treatment. Each figure representative of at least two independent experiments. Student's t-test was used to compare two groups.

Figure S 3
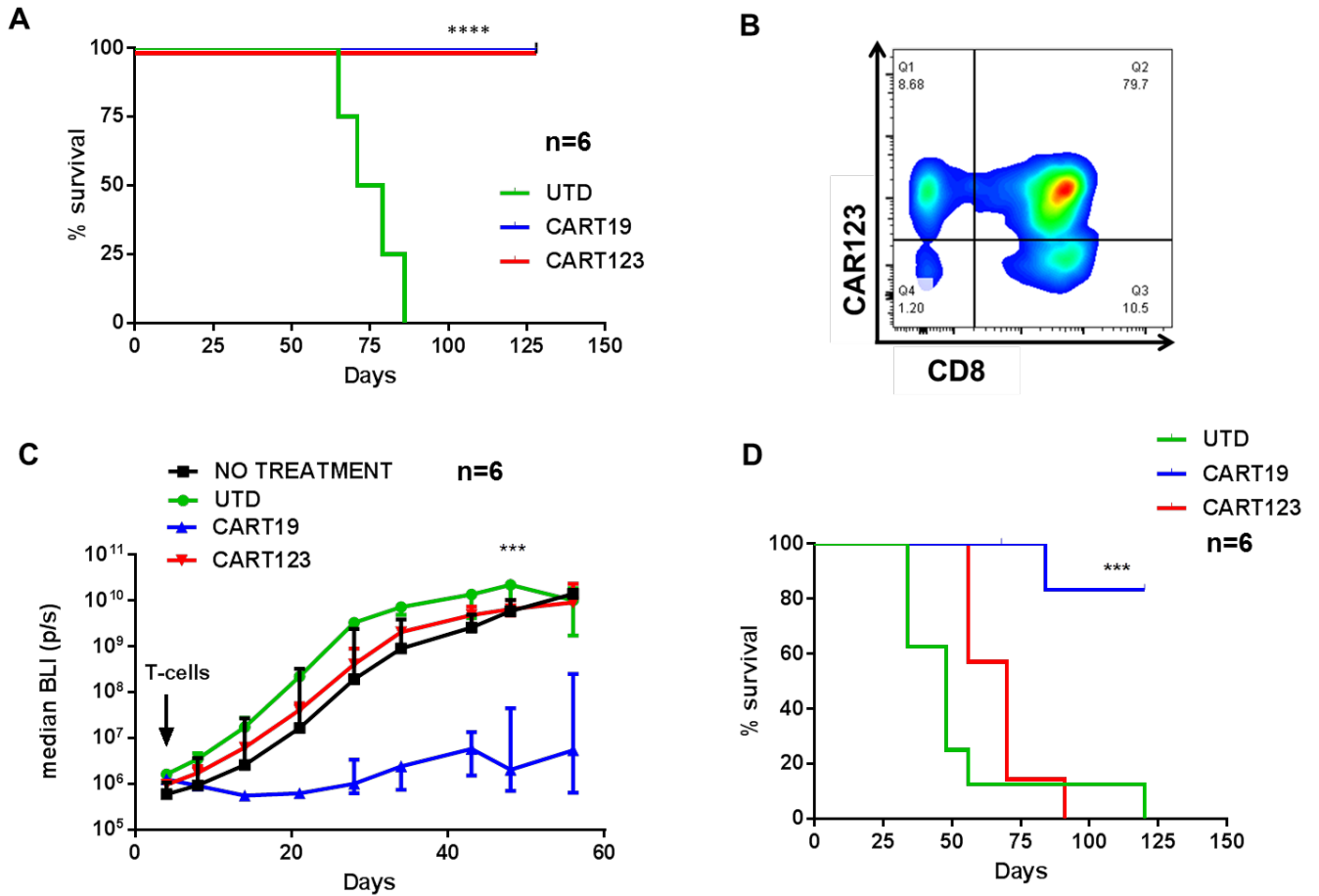
Figure S3. In vivo xenograft models of primary leukemia. A. CD19+ CD123+ luciferase+ primary B-ALL blasts (UPN#11) were injected in NSG mice and after 14 days mice were randomized based on tumor burden to receive either CART123, CART19 or control T cells (UTD). Mice receiving CART123 or CART19, but not UTD, showed a significant advantage in overall survival. **B.** Peripheral blood (PB) flow cytometry analysis of leukemic mice receiving anti-CD123 chimeric antigen receptor T cells (CART123). Human T cells (CD8+ and CD8-) can be detected in the PB with the majority of them being CAR123+. **C.** CD123- CD19+ luciferase+ primary B-ALL blasts (a rare finding) were injected in NSG mice and after 7 days mice were randomized based on tumor burden (bioluminescence) to receive either CART123, CART19, control T cells (UTD) or no treatment. Mice receiving CART19 but not CART123 nor UTD, showed quick leukemia remission that was maintained at long term leading to a significant advantage in overall survival (median survival not reached for CART19 vs 70 days for CART123, p=0.0002) **(D)**. All graphs representative of two independent experiments (6 mice per group). Student's t-test or ANOVA for each time points/ratios was used. Survival curves were compared using the log-rank test.

Figure S 4
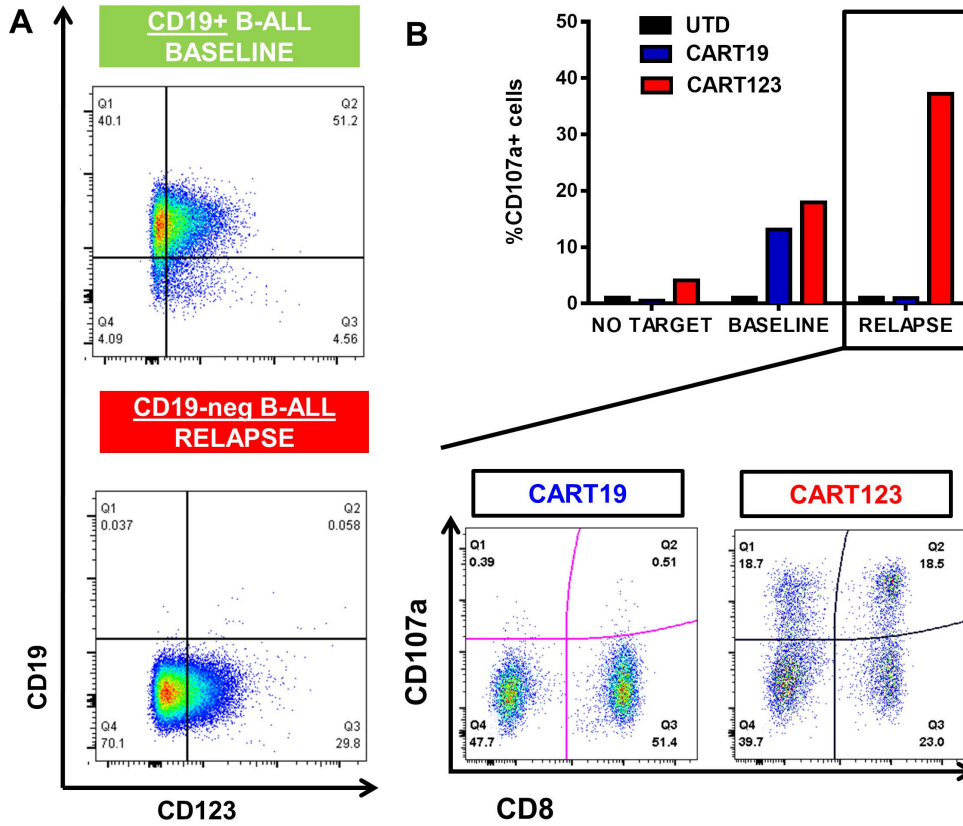
Figure S4. In vitro activity of anti-CD123 CART against CD19-negative ALL. A. Blasts from a pediatric patient (UPN#09) were collected at baseline (top) and at relapse (bottom). Expression of CD19 and CD123 was analyzed by flow cytometry. CD19 is expressed at baseline but it is completely lost at relapse instead CD123, although dim, is expressed at the same level at relapse. **B.** A CD107a degranulation assay was performed co-culturing UTD, CART19 and CART123 with UPN#09 blasts from baseline or relapse (no target as a control). Only CART123 cells, both CD8+ and CD8-, were able to degranulate when co-cultured with either baseline or relapsed blasts while CART19 is only reactive to baseline blasts, indicating that CART123 can be effective in recognizing CD19-negative relapsed leukemia.
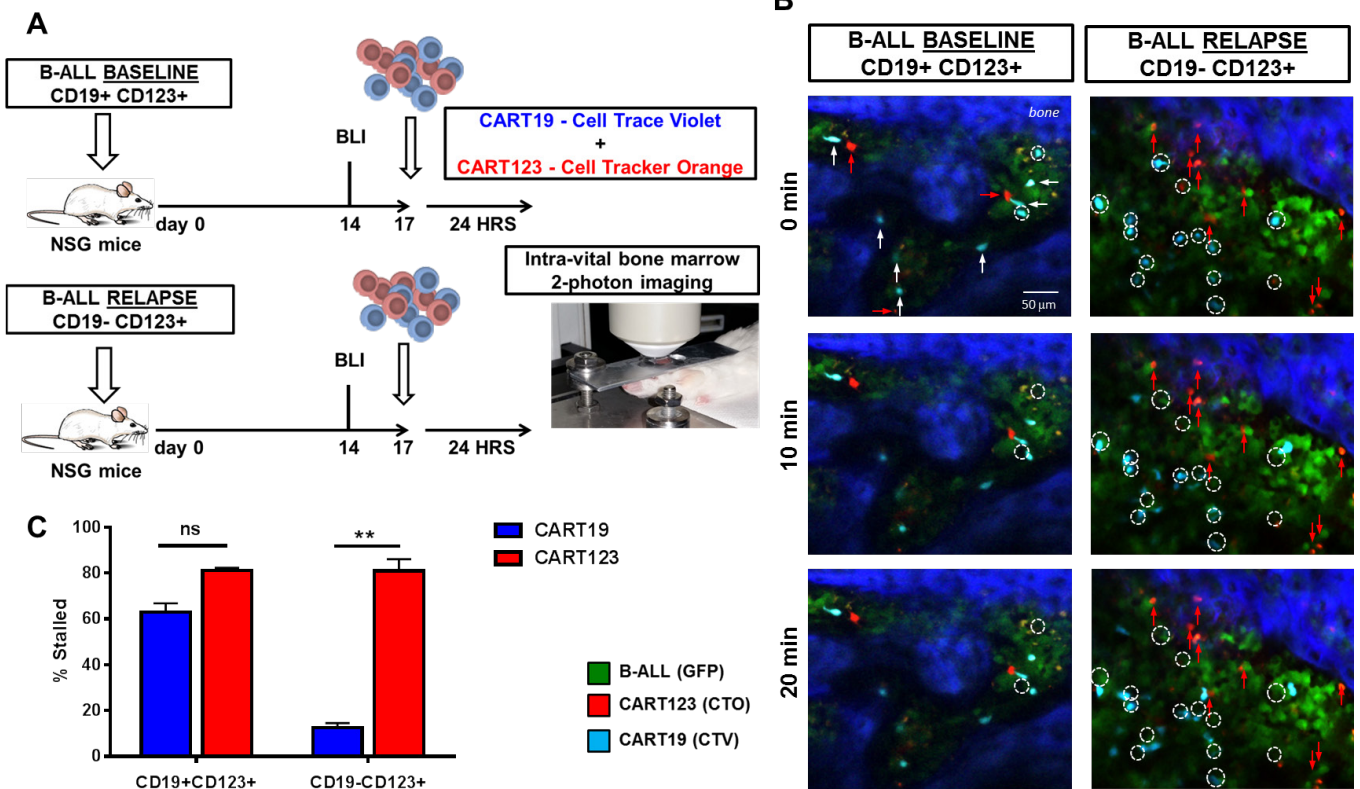
Figure S5: Multiphoton microscopy of B-ALL-CART interactions in skull bone marrow of xenograft mice. A. Experiment schema; two groups of NSG mice were respectively engrafted with B-ALL blasts (GFP+) originally obtained from a patient (UPN#09) at baseline and at CD19- relapse. At day 17 mice of both groups were randomized to receive a 1:1 mixture of CART123 and CART19 cells that were previously labeled with two different dyes (CTV-Cell Trace Violet or CTO-Cell Tracker Orange). After twenty-four hours mice were anesthetized and the skull was exposed and prepared for 2-photon microscopic analysis. **B.** Representative multiphoton XY plane images of CART19 cells (blue) and CART123 cells (red) interacting with B-ALL blasts (green) from baseline (left) (CD19+ CD123-) and at antigen-loss relapse (right) (CD19- CD123+). The bone is also imaged using second harmonic generation at 425 nm (dark blue). CART19 cells that are motile are indicated using white dashed circles. CART19 and CART123 cells that are non-motile are indicated using white and red arrows, respectively. In the presence of baseline leukemia both CART19 and CART123 cells are non-motile and globular indicating the formation of productive synapse with the leukemic blasts. Instead in the presence of relapsed leukemia, CART19 cells are motile and spindle-shaped indicating that they cannot recognize the blasts; CART123 instead are non-motile and globular indicating that are recognizing the leukemic blasts. **C.** Percentage of non-motile CART19 and CART123 cells in the two groups. CART19 cells are significantly more motile in mice engrafted with CD19- ALL, while CART123 cell motility is unchanged between tumor types. (Baseline ALL: n = 2 mice, 204 CART19 and 208 CART123 cells analyzed; Relapsed ALL: n = 3 mice, 176 CART19 and 109 CART123 cells analyzed). Student's t-test was used to compare two groups.

Figure S 6
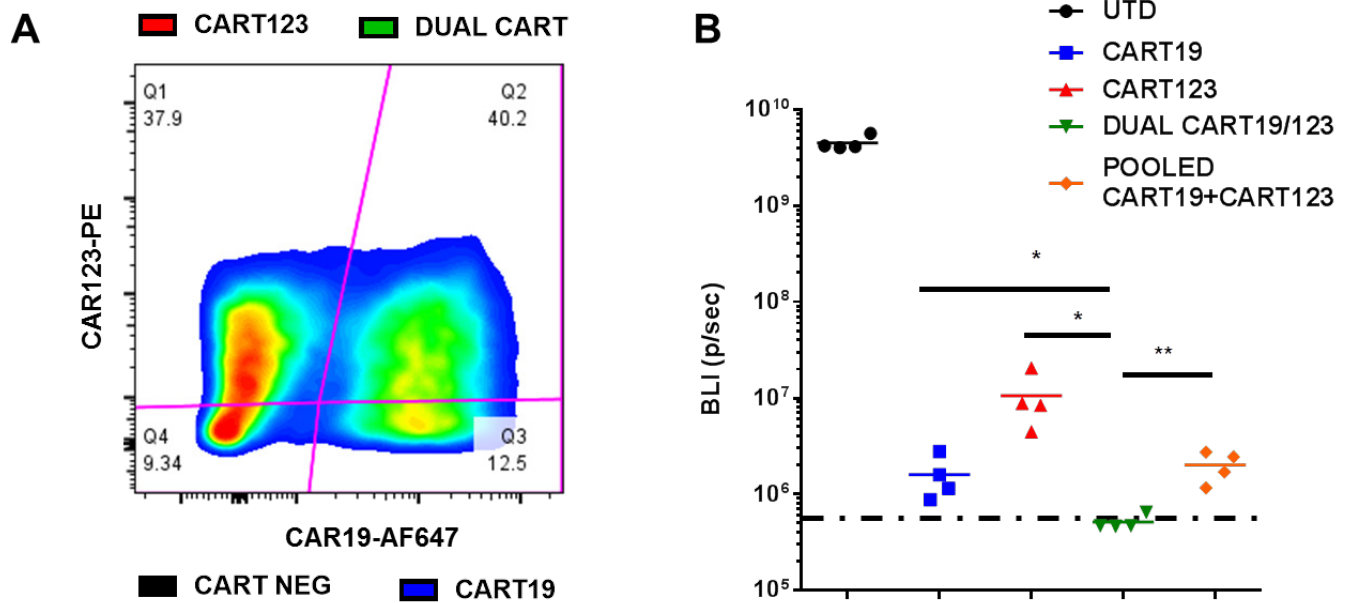
Figure S6: CD19-negative relapse animal model and dual CART. A. T cells were expanded according to our standard protocol and transduced using two lentiviruses carrying respectively CAR19 and CAR123 (multiplicity of infection, MOI=3). Four distinct populations based on the specific expression of CAR19 and/or CAR123 can be recognized, including a Dual CAR19+/CAR123+ population. These four populations were sorted and a CD107a degranulation experiment was performed. **B.** NSG mice were engrafted with a B-ALL cell line (NALM-6, CBG+). At day 7 mice were randomized based on tumor burden (BLI, bioluminescence) to receive control T cells (UTD), CART19, CART123, the 1:1 pooled combination of CART123 and CART19 or the Dual CART19/123 (same total number of CAR+ cells). The tumor burden 6 days after T cell infusion (day 13) is shown in the graph: the deepest short term anti-leukemia response is observed in the dual CART group. Student's t-test was used to compare two groups; in analysis where multiple groups were compared, one-way analysis of variance (ANOVA) was performed with Holm-Sidak correction for multiple comparisons.

Movie S1: Multiphoton microscopy of leukemia-CAR T cell interactions in skull bone marrow of mice xenografted with baseline leukemia (CD19+ CD123+). CART19 (blue cells) cells and CART123 (red) cells interacting with B-ALL (green) from patient UPN#09 from baseline (CD19+ and CD123+). The bone is also imaged using second harmonic generation at 425 nm (dark blue). In the presence of baseline leukemia both CART19 and CART123 cells are non-motile and with a globular shape, indicating the formation of productive synapses with the leukemic blasts.

Movie S2: Multiphoton microscopy of leukemia-CAR T cell interactions in skull bone marrow of of mice xenografted with relapsed leukemia (CD19- CD123+). CART19 (blue cells) cells and CART123 (red) cells interacting with B-ALL (green) from patient UPN#09 at antigen-loss relapse (CD19- CD123+). The bone is also imaged using second harmonic generation at 425 nm (dark blue). In the presence of relapsed leukemia CART19 cells are highly motile and spindle-shaped indicating that do not encounter recognized targets; CART123 instead are non-motile and with globular shape indicating that are recognizing the leukemic blasts.

Table S1. **Flow cytometry antibodies and reagents used for the present study.**

Specificity	fluorochrome	clone	vendor	cat #
CAR19	CD19-Fc/His		SinoBiologicals	11880-H08H-50
CAR19	AF647	136.20.1	NA	NA
CAR123	CD123-Fc/His		SinoBiologicals	10518-H03H-50
CD107a	PE-Cy7	H4A3	Biolegend	328618
CD10	BV421	HI10a	Biolegend	312218
CD123	PE	6H6	eBioscience	12-1239-42
CD123	PECY7	6H6	eBioscience	25-1239-42
CD14	V500	M5E2	BD Horizon	561391
CD19	PE-Cy7	SJ25C1	eBioscience	25-0198-42
CD19	PerCP Cy5.5	HIB19	Biolegend	302230
CD19	PE	HIB19	eBioscience	12-0088-42
CD19	APC	HIB19	eBioscience	17-0199-42
CD20	PECY7	2H7	eBioscience	25-0209-42
CD22	PE	HIB22	BioLegend	302506
CD22	PECY7	HIB22	BioLegend	302514
CD3	PE-Cy7	UCHT1	eBioscience	25-0038-42
CD3	PE	OKT3	eBioscience	12-0037-42
CD3	BV711	OKT3	BioLegend	317328
CD34	APC	4H11	eBioscience	17-0349-42
CD38	BV711	HIT2	BioLegend	303528
CD38	PECY7	HIT2	BioLegend	25-0389-42
CD4	BV605	OKT4	Biolegend	317438
CD45	BV421	HI30	Biolegend	304032
CD8	BV605	RPA-T8	Biolegend	301040
CD8	PE-Cy7	RPA-T8	eBioscience	25-0088-42
GM-CSF	BV421	BVD2-21C11	BD Biosciences	562930
IFNgamma	PE	4S.B3	BioLegend	502509
IL-2	PECF594	5344.111	BD Biosciences	562384

TNF-a	AF700	Mab11	BioLegend	502928
murine CD45	APC Cy7	30-F11	Biolegend	103116
MIP-1b	PE-CY7	D21-1351	BD Biosciences	560687
LiveDead Aqua	NA	NA	ThermoFisher	L34957